

Electron-induced excitation of vibrations of Ce atoms inside a C₈₀ cageA. Stróżecka,^{1,2,*} K. Muthukumar,^{3,†} J. A. Larsson,³ A. Dybek,⁴ T. J. S. Dennis,⁴ J. Mysliveček,⁵ and B. Voigtländer¹¹*Peter Grünberg Institut (PGI-3), and JARA, Fundamentals of Future Information Technology, Forschungszentrum Jülich, D-52425 Jülich, Germany*²*Institut für Experimentalphysik, Freie Universität Berlin, Arnimallee 14, D-14195 Berlin, Germany*³*Tyndall National Institute, University College Cork, Lee Maltings, Prospect Row, Cork, Ireland*⁴*Department of Physics, Queen Mary, University of London, Mile End Road, London E1 4NS, United Kingdom*⁵*Charles University, Faculty of Mathematics and Physics, V Holešovičkách 2, Praha 8, Czech Republic*

(Received 15 June 2010; revised manuscript received 2 February 2011; published 14 April 2011)

Inelastic electron tunneling spectroscopy of Ce₂@C₈₀ dimetallofullerenes reveals a low-energy inelastic excitation that is interpreted using *ab initio* calculations and associated with the movements of encapsulated Ce atoms inside the C₈₀ cage. The electron-vibration interaction in Ce₂@C₈₀ is unusually high, inducing a pronounced zero-bias anomaly in differential conductance of Ce₂@C₈₀. Our observations show that the atoms encapsulated in fullerene cages can actively participate in determining the properties of molecular junctions.

DOI: 10.1103/PhysRevB.83.165414

PACS number(s): 82.37.Gk, 71.20.Tx, 73.63.Rt

I. INTRODUCTION

Electron-vibration interactions are known to influence the properties of single-molecule electronic junctions¹ like the current-to-voltage characteristics² or the current limit.³ Experimentally, electron-vibration interactions are often studied in model single-molecule junctions realized in scanning tunneling microscope (STM) where one electrode (the STM tip) is connected to the molecule/counter electrode setup via a tunneling gap. In such junctions, the opening of inelastic tunneling channels allows the detection of single-molecule vibrations through inelastic electron tunneling spectroscopy (IETS).⁴

Fullerenes represent prototypical molecules for single-molecule junction studies. For the single C₆₀ the stability,³ the conductance,^{5,6} and the electron-vibration fingerprint in different junction geometries^{2,7,8} have been thoroughly studied. Functionality of empty fullerene cages is expected to become significantly more complex on endohedral doping, when atoms or molecules are enclosed in the carbon cages of fullerenes.⁹ A study of Ce₂@C₈₀ showed that the doping directly influences the conductance of the corresponding molecular junction.¹⁰ Generally, the atoms and molecules inside the fullerene cages are very well screened from the external physical and chemical influences.^{11,12} As a consequence, no vibration excitations of the encapsulated atoms were found in previous single-molecule electronic junction studies on endofullerenes.¹³

Here we present evidence for the electron-vibration excitation of Ce atoms engaged in a C₈₀ fullerene (Ce₂@C₈₀). Inelastic electron tunneling spectroscopy together with *ab initio* calculations indicate that the lowest-energy excitations in the IETS spectrum of Ce₂@C₈₀ represent the vibrations of Ce atoms inside the C₈₀ cage. The endohedral doping of Ce₂@C₈₀ also contributes to enhancing the overall cross section of the electron-vibration excitation in the molecular junction. We observe a massive increase of the tunneling conductance by a factor of 2 in the energy range of the excited vibrations, leading to a pronounced zero-bias conductance anomaly and a distinct nonlinearity in the current-to-voltage characteristics of the single-molecule junction. Our experiments

show that the atoms inside fullerene cages can significantly influence the characteristics of the corresponding molecular junctions.

II. EXPERIMENTAL

The experiments were performed with a commercial ultra-high vacuum STM operated at $T = 6$ K. Ce₂@C₈₀ metallofullerenes were isolated from soot by high-performance liquid chromatography (HPLC) as described in Ref. 14. Cu(111) substrates were cleaned by repeated cycles of Ne⁺ sputtering and vacuum annealing. Ce₂@C₈₀ molecules were evaporated from a Knudsen cell on a clean Cu(111) surface held at room temperature. Experiments with Ce₂@C₈₀ on Cu(111) were complemented by reference measurements with Ce@C₈₂ (Refs. 14 and 15) and C₆₀ (Ref. 10) on Cu(111) and with Ce₂@C₈₀ on Au(111).

STM measurements were performed with electrochemically etched W tips treated by interactions with the Cu(111) substrate until delivering tunneling spectra corresponding to clean Cu(111).¹⁰ Measurements of the current-to-voltage (I/V) characteristic of the tunneling junctions and their first (dI/dV) and second (d^2I/dV^2) derivatives were performed at a constant tip-sample separation given by the set current $I_0 = 0.5$ nA and the set sample bias $V_0 = 150$ mV before switching off the feedback of the STM. dI/dV and d^2I/dV^2 were measured by two lock-in amplifiers using bias voltage modulation with the frequency of ≈ 360 Hz and the rms amplitude 6 mV. We realized and analyzed about 80 single-molecule junctions with Ce₂@C₈₀.

III. IETS OF CE₂@C₈₀

The schematic of the adsorption of Ce₂@C₈₀ on Cu(111) is shown in Fig. 1(a). The Ce atoms are enclosed in the I_h isomer of the C₈₀ cage.¹⁴ The adsorption geometry with the six-membered ring parallel to the surface and the positions of the Ce atoms in the adsorbed molecule have been established by previous calculations.^{10,16} On deposition at room temperature (RT), Ce₂@C₈₀ nucleate in small islands on Cu(111) planes. A detail of such island is shown in the STM image in Fig. 1(b).

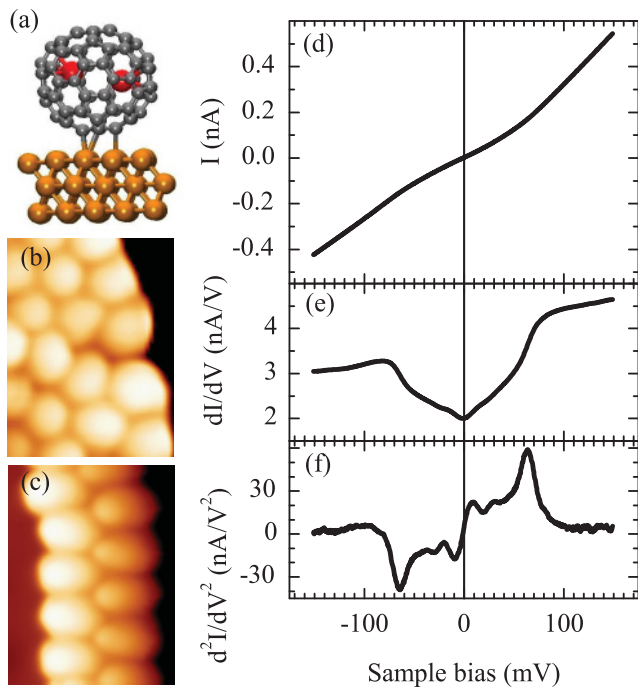


FIG. 1. (Color online) $\text{Ce}_2@C_{80}$ molecules adsorbed on the Cu(111) surface. (a) Schematic, (b) STM image after deposition at RT, and (c) annealed to 250 °C. Image width in (b) and (c) is 4 nm. [(d)–(f)] A pronounced fingerprint of the electron-vibration excitations of $\text{Ce}_2@C_{80}$ in the I/V characteristic of the tunneling junction and its derivatives.

The adsorption position of $\text{Ce}_2@C_{80}$ can be modified by annealing to 250 °C, after which the molecules decorate the step edges of Cu(111) as shown in the STM image in Fig. 1(c). Regardless of the sample bias applied, $\text{Ce}_2@C_{80}$ reveal no intramolecular structure and always appear in the images as featureless protrusions, in contrast to C_{60} on Cu(111).^{10,17}

A typical IETS of the $\text{Ce}_2@C_{80}$ is shown in Figs. 1(d)–1(f). The I/V curve [Fig. 1(d)] shows a visible nonlinearity—a decrease of the differential conductance in the proximity of zero bias. In dI/dV , a pronounced zero-bias conductance anomaly becomes apparent [Fig. 1(e)]. Finally, the d^2I/dV^2 [Fig. 1(f)] shows pronounced symmetric peaks and dips characteristic of inelastic electron tunneling.¹⁸ Each peak corresponds to opening of one of several inelastic electron tunneling channels with increasing bias voltage. We attribute the inelastic losses to the excitation of molecular vibrations of $\text{Ce}_2@C_{80}$. The distinct influence of the electron-vibration excitation on the I/V curve of the molecular junction indicates an unusually high cross section of this process.

In the voltage region of a few millielectron volts, d^2I/dV^2 curves measured on molecules often exhibit features lacking the necessary symmetry and/or show too much correlation to the d^2I/dV^2 curve of the bare substrate to qualify for electron-vibration excitations. We revisit the lowest-energy d^2I/dV^2 peaks of the $\text{Ce}_2@C_{80}$ molecule on a detailed view in Fig. 2. We observe that these peaks do have the symmetry required for the qualification as inelastic excitations. A comparison to the

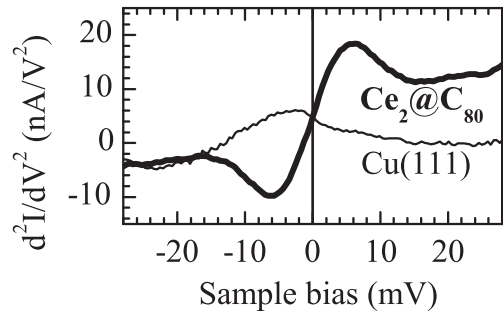


FIG. 2. Detail of d^2I/dV^2 curve measured over a $\text{Ce}_2@C_{80}$ molecule (thick line) compared to a bare Cu(111) substrate (thin line). The symmetry and the absence of substrate-related features classifies the d^2I/dV^2 measured over the molecule as a fingerprint of a low-energy electron-vibration excitation.

d^2I/dV^2 curve measured on the bare substrate also shows that the lowest-energy vibrations are a property of the $\text{Ce}_2@C_{80}$ molecule and not an artifact from the STM tip and/or from the substrate.

The conductance anomaly as shown in Fig. 1(e) is observed for all investigated $\text{Ce}_2@C_{80}$ molecules. A selection of d^2I/dV^2 curves illustrating the common features and the differences of the individual molecular junctions is shown in Fig. 3. In each d^2I/dV^2 curve, we mark the positions of the peaks that have an antisymmetric counterpart and thus correspond to a vibration excitation. Common to all junctions are the excitations between 6 and 11 meV (Ref. 19) and between 60 and 65 meV. We label these excitations ν_1 and ν_2 , respectively. Apart from ν_1 and ν_2 , up to three excitations with intermediate or higher energies are present. The observation of ν_1 and ν_2 is robust: they are observed for $\text{Ce}_2@C_{80}$ on Cu(111) deposited at RT [Figs. 3(a)–3(c)] as well as annealed to 250 °C [Figs. 3(d)–3(f)], and in a reference experiment with $\text{Ce}_2@C_{80}$ deposited at RT on Au(111) [Fig. 3(g)]. Especially, the ν_1 represents an excitation characteristic of the $\text{Ce}_2@C_{80}$ molecule. This has been confirmed by further reference experiments: the ν_1 is absent in C_{60} on Cu(111) and single-doped metallofullerene $\text{Ce}@C_{82}$ molecules on Cu(111). ν_1 and ν_2 exhibit small, and the other observed vibrations somewhat larger variations of energy and amplitude which we attribute to the availability of different adsorption sites,¹⁰ varying numbers of neighboring $\text{Ce}_2@C_{80}$ molecules, and variations caused by a strong localization of the IETS signal over a single fullerene cage.¹³ Calculating the normalized change in the differential conductance, defined as $\Delta\sigma/\sigma$, where $\sigma = dI/dV$,²⁰ we obtain electron-vibration cross sections 15–20% for ν_1 , 30–40% for ν_2 , and 5–15% for other observed excitations. The values for ν_1 and ν_2 exceed the values commonly observed in the IETS experiments on fullerenes^{7,13} and other molecules²⁰ that stay below 15%.

The unambiguous (cf. Fig. 2) and intensive low-energy excitation has not been observed in previous STM-IETS studies on empty fullerenes (C_{60} in Refs. 7 and 17) and endohedrally doped fullerenes ($\text{Gd}@C_{82}$ in Ref. 13). We will discuss the nature of this highly intriguing IETS feature based on *ab initio* calculations of electron-vibration coupling in $\text{Ce}_2@C_{80}$. In the discussion we rule out the possibility

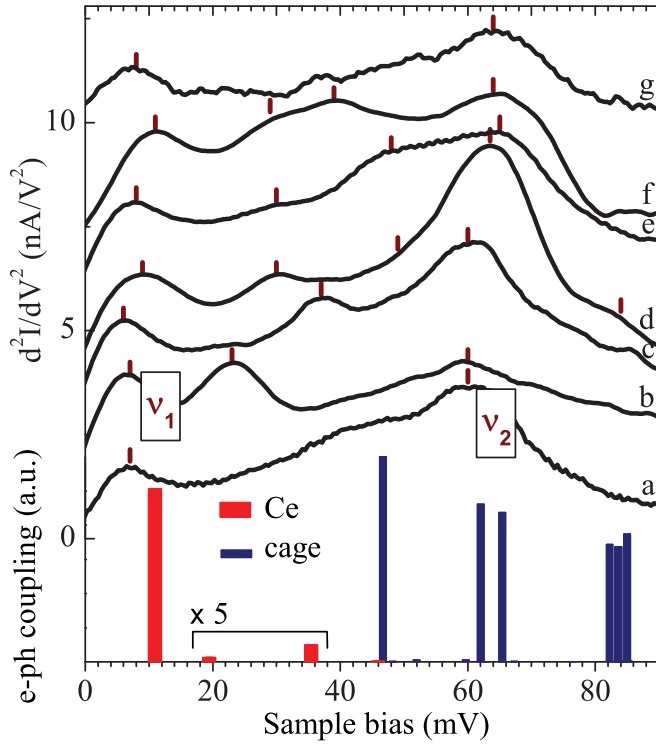


FIG. 3. (Color online) d^2I/dV^2 vibration spectra of $Ce_2@C_{80}$ molecules [(a)–(c)] on Cu(111), deposited at RT, [(d)–(f)] on Cu(111), annealed to 250 °C, (g) on Au(111), deposited at RT. Peaks corresponding to vibrations are marked by vertical bars. Vibrations common to all observed molecules between 6 and 11 meV and between 60 and 65 meV are labeled ν_1 and ν_2 , respectively. The bar graph shows electron-vibration coupling calculated for the vibration modes of a free $Ce_2@C_{80}$ molecule. Vibrations that involve movements of Ce atoms are shown in red (broad bars).

that the low-energy excitation is due to molecule-substrate movements (bouncing). Observation of bouncing in fullerenes has been limited to non-STM IETS experimental setups so far (C_{60} in Ref. 2). Rather, we propose that the ν_1 is due to movements of Ce with respect to the C_{80} cage. Our proposal is based on the observation that the Ce-cage vibration modes occupy the lowest energies in the Raman spectra of endohedral metallofullerenes.^{21,22}

IV. CALCULATION OF CE VIBRATIONS

In the following, we are discussing the observed vibrations based on the results of ab-initio calculations. We evaluate the cross section for exciting an inelastic electron-vibration tunneling channel as

$$\Delta\rho_i \approx \left| \frac{dE_{E_F}}{dQ_i} \frac{\hbar}{\sqrt{2m_i^*\Omega_i}} \right|^2, \quad (1)$$

where E_{E_F} is the energy of a molecular orbital inelastically coupling at the Fermi level, and Q_i , m_i^* , and Ω_i are the normal coordinate, the reduced mass, and the frequency of the i^{th} molecular vibration, respectively. Equation (1) represents a useful approximation for discussing the IETS of endofullerenes.¹³ In order to make the *ab initio* analysis

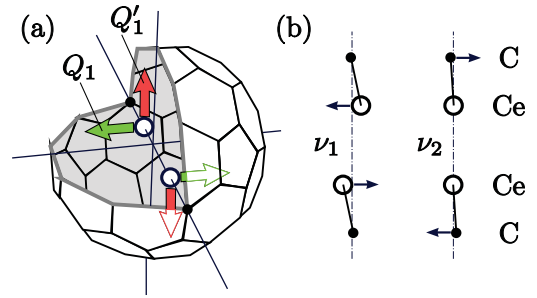


FIG. 4. (Color online) (a) Schematic of the Ce motions inside the C_{80} cage corresponding to the ν_1 electron-vibration excitation. The ν_1 has e_g symmetry, is twofold degenerate (Q_1 , Q_1'), and involves motions of Ce atoms parallel to the C cage. (b) Displacements of atoms on the C–Ce–Ce–C axis for ν_1 at 11 meV and ν_2 at 65 meV. The positions of the atoms correspond to the calculated turning point of the vibration; the arrows indicate the direction of the atom motion.

feasible, we calculated the electron-vibration cross sections of a free $Ce_2@C_{80}$. We used unrestricted density functional theory (DFT) as implemented in TURBOMOLE 5.10.²³ Details of the calculations are given in a previous work where the ground state and the infrared (IR) vibration spectrum of $Ce_2@C_{80}$ have been determined.¹⁶ The derivative of the highest occupied molecular orbital (HOMO) energy with respect to Q_i (dE_{E_F}/dQ_i) was calculated numerically, displacing the atoms by 0.05 Å in directions given by Q_i and evaluating the corresponding change of the HOMO energy.²⁴

The calculated energies of the vibration modes of $Ce_2@C_{80}$ and the electron-vibration coupling with the HOMO of the molecule are plotted as a bar graph in Fig. 3. The calculations predict 58 vibration modes in the energy range up to 90 meV. Of these modes, only some are electron-vibration active, but of the active modes several have a significant contribution from Ce movements. We distinguish the vibration modes based on their effective mass m_i^* : the modes with $m_i^* > 12.5$ (compared to 12.011 for pure carbon cage modes) are considered Ce active. In Fig. 3 these modes are shown in red.

V. DISCUSSION

The calculations indicate that the experimentally observed vibration ν_1 can be identified with a theoretically predicted inelastic excitation with an energy of 11 meV. This excitation involves Ce motions inside the C_{80} cage (cf. Fig. 3). We show the schematic of the ν_1 vibration as obtained from the *ab initio* calculations in Fig. 4(a). ν_1 is twofold degenerate, has e_g symmetry, and involves the motions of Ce atoms perpendicular to the C–Ce–Ce–C axes (parallel to the C_{80} cage). The calculated Ce vibration modes at higher energies have a significantly lower electron-vibration activity. The mode at 19 meV has a_{1g} symmetry and represents Ce–Ce stretching. A mode with the same symmetry has been identified as the lowest-energy mode in $La_2@C_{80}$.²⁵ The mode at 35 meV has a_{1g} symmetry as well and includes Ce–C

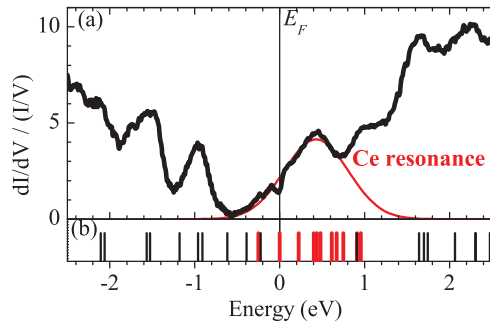


FIG. 5. (Color online) (a) Density of electron states of the $\text{Ce}_2@C_{80}$ molecule measured by STS. The Ce resonance is crossing the Fermi level. The red curve is a fit to the experimental data. (b) Calculated electron states of a free $\text{Ce}_2@C_{80}$ molecule. States with a $>80\%$ Ce contribution are marked red (broad bars). The Ce-dominated states have energies between $(-0.2, 1.2)$ eV, and include both the HOMO and the LUMO of the molecule. The Ce-dominated states form a resonance near E_F also in an adsorbed molecule.¹⁰

stretching along the C–Ce–Ce–C axis (perpendicular to the C_{80} cage).

Calculated cage vibration modes appear at energies ≥ 27 meV. However, a significant electron-vibration cross section is calculated only for cage modes at energies ≥ 47 meV. The electron-vibration excitations at 62 and 65 meV correspond to the experimental peak ν_2 . The assignment of the smaller experimental vibration peaks between ν_1 and ν_2 , and above ν_2 , to the calculated Ce and/or cage modes is less straightforward. Particularly, strong calculated modes at 47 and 85 meV are marginal in the experimental IETS, which may reflect differences between the free (calculation) and the adsorbed molecule (experiment).

The unusually high cross section for the electron-vibration excitation in $\text{Ce}_2@C_{80}$ can be traced back to a coincidence of favorable conditions enhancing the IETS signal that is related to the unique electron structure of $\text{Ce}_2@C_{80}$. In Ref. 10 we have shown that orbitals of the encapsulated Ce atoms localize strongly both in space and in energy and that they separate both in space and energy from the cage orbitals. This situation is illustrated in Fig. 5 where we plot the density of states (DOS) of the adsorbed molecule as measured by STS [Fig. 5(a)] and the electron levels of a free molecule from the present calculation [Fig. 5(b)].²⁶ In the calculated data, we mark the electron levels of orbitals with $>80\%$ Ce contribution red. We observe that the Ce orbitals form a multiplet at and above the E_F , approximately between 0 and 1 eV. The cage orbitals, on the other hand, are observed exclusively outside this energy range. This allows us to identify and fit the Ce resonance in the experimental STS data [red line in the Fig. 5(a)].

Generally, the position of the molecular resonance participating in the inelastic tunneling with respect to E_F is a main factor determining the sign and the size of the inelastic conductivity change.^{27,28} Experiments on C_{60} show that the IETS cross section becomes maximized, when the molecular resonance is tailing E_F .⁸ This is the case for the Ce resonance in our experiment [Fig. 5(a)] and the first favorable condition

for the high IETS cross section in $\text{Ce}_2@C_{80}$. The strength of the electron-vibration interaction further increases with decreasing molecule-electrode coupling.^{1,29} In recent conductivity measurements on single $\text{Ce}_2@C_{80}$, we have demonstrated that for the localized Ce orbitals the molecule-electrode coupling is significantly reduced,¹⁰ which represents the second favorable condition for a large IETS cross section. Finally, the multiplet character of the Ce resonance in $\text{Ce}_2@C_{80}$ may contribute to establishing of inelastic transmission channels for many different contact geometries and thus to weakening the restrictions to the availability of such channels that can be imposed by the symmetry of the electrodes in the single-molecule contact.^{1,30}

The Ce vibration modes at 11 meV (ν_1) and 35 meV induce movements of Ce atoms in different directions with respect to the C_{80} cage. Mutual Ce–C movements are observed also for the cage modes at higher energy. An example is displayed in Fig. 4(b) where the cage vibration at 65 meV (ν_2) induces displacements of C atoms perpendicular to the C–Ce–Ce–C axis, complementary to the movements observed in the ν_1 mode. We can speculate that in the low-temperature STM IETS the highly effective electron-vibration excitation of ν_1 and higher-energy vibrations induces hopping of Ce atoms between the equivalent positions inside the C_{80} cage. Such hopping of endohedral atoms inside the C_{80} cage has been reported to appear spontaneously in $\text{La}_2@C_{80}$ at room temperature³¹ when the activation energy for hopping in the order of tens of millielectron volts (Ref. 25) is supplied by thermal fluctuations.

VI. CONCLUSIONS

We are presenting inelastic electron tunneling spectroscopy of single $\text{Ce}_2@C_{80}$ molecules in scanning tunneling microscope together with *ab initio* analysis of electron-vibration coupling in $\text{Ce}_2@C_{80}$. We are observing a low-energy inelastic tunneling excitation in $\text{Ce}_2@C_{80}$ that can be interpreted as excitation of movements of encapsulated Ce atoms inside C_{80} cage. The Ce-cage vibration and pure cage vibrations in $\text{Ce}_2@C_{80}$ exhibit a very high electron-vibration coupling resulting in a pronounced zero-bias conductance anomaly in STM-IETS of $\text{Ce}_2@C_{80}$. We trace this unique behavior of $\text{Ce}_2@C_{80}$ back to its electron structure, where the orbitals localized on the Ce atoms are forming a strong band at energies between 0 and 1 eV above E_F , and mediate the electron-vibration interactions in $\text{Ce}_2@C_{80}$. Our observations show that encaged atoms can significantly influence the dynamics of fullerene-based molecular junctions.

ACKNOWLEDGMENTS

This work was supported by the FP6 Marie Curie Early Stage Training Network NANOCAGE (MEST-CT-2004-50-6854), Science Foundation Ireland, and the Ministry of Education of the Czech Republic (MSM 0021620834). We acknowledge the SFI/HEA Irish Centre for High-End Computing (ICHEC) for generous allotment of computer resources. We thank J. I. Pascual and K. J. Franke for many helpful discussions.

*anna.strozecka@physik.fu-berlin.de

†Present address: Department of Chemical and Materials Engineering, University of Cincinnati, Cincinnati, 45220 OH, USA.

- ¹M. Galperin, M. A. Ratner, A. Nitzan, and A. Troisi, *Science* **319**, 1056 (2008).
- ²H. Park, J. Park, A. K. L. Kim, E. H. Anderson, A. P. Alivisatos, and P. L. McEuen, *Nature* **407**, 57 (2000); L. H. Yu and D. Natelson, *Nano Lett.* **4**, 79 (2004).
- ³M. Galperin, M. A. Ratner, and A. Nitzan, *J. Phys. Condens. Matter* **19**, 103201 (2007); G. Schulze, K. J. Franke, and J. I. Pascual, *New J. Phys.* **10**, 065005 (2008).
- ⁴B. C. Stipe, M. A. Rezaei, and W. Ho, *Science* **280**, 1732 (1998).
- ⁵C. Joachim, J. K. Gimzewski, R. R. Schlittler, and C. Chavy, *Phys. Rev. Lett.* **74**, 2102 (1995).
- ⁶N. Neél, J. Kröger, L. Limot, T. Frederiksen, M. Brandbyge, and R. Berndt, *Phys. Rev. Lett.* **98**, 065502 (2007); N. Neél, J. Kröger, L. Limot, and R. Berndt, *Nano Lett.* **8**, 1291 (2008).
- ⁷J. I. Pascual, J. Gómez-Herrero, D. Sánchez-Portal, and H. P. Rust, *J. Chem. Phys.* **117**, 9531 (2002).
- ⁸K. J. Franke, G. Schulze, and J. I. Pascual, *J. Phys. Chem. Lett.* **1**, 500 (2010).
- ⁹H. Shinohara, *Rep. Prog. Phys.* **63**, 843 (2000).
- ¹⁰A. Stróżecka, K. Muthukumar, A. Dybek, T. J. Dennis, J. A. Larsson, J. Mysliveček, and B. Voigtländer, *Appl. Phys. Lett.* **95**, 133118 (2009).
- ¹¹P. Delaney and J. C. Greer, *Appl. Phys. Lett.* **84**, 431 (2004); K. Schulte, L. Wang, P. J. Moriarty, J. Purton, S. Patel, H. Shinohara, M. Kanai, and T. J. S. Dennis, *Phys. Rev. B* **71**, 115437 (2005).
- ¹²W. Harneit, *Phys. Rev. A* **65**, 032322 (2002).
- ¹³M. Grobis, K. H. Khoo, R. Yamachika, X. Lu, K. Nagaoka, S. G. Louie, M. F. Crommie, H. Kato, and H. Shinohara, *Phys. Rev. Lett.* **94**, 136802 (2005).
- ¹⁴M. Kanai, T. J. S. Dennis, and H. Shinohara, *Am. Inst. Phys. Conf. Proc.* **633**, 35 (2002).
- ¹⁵L. Wang, K. Schulte, R. A. J. Woolley, M. Kanai, T. J. S. Dennis, J. Purton, S. Patel, S. Gorovikov, V. R. Dhanak, E. F. Smith, B. C. C. Cowie, and P. Moriarty, *Surf. Sci.* **564**, 156 (2004).
- ¹⁶K. Muthukumar and J. A. Larsson, *J. Mater. Chem.* **18**, 3347 (2008).
- ¹⁷J. A. Larsson, S. D. Elliott, J. C. Greer, J. Repp, G. Meyer, and R. Allenspach, *Phys. Rev. B* **77**, 115434 (2008); A. Stróżecka, J. Mysliveček, and B. Voigtländer, *Appl. Phys. A* **87**, 475 (2007).
- ¹⁸W. Ho, *J. Chem. Phys.* **117**, 11033 (2002).
- ¹⁹Technically, 6 mV is the lowest-energy peak that can be obtained from IETS measurement with 6-mV rms modulation. The actual energy of the corresponding inelastic excitation may eventually be lower.
- ²⁰B. C. Stipe, M. A. Rezaei, and W. Ho, *Rev. Sci. Instr.* **70**, 137 (1998).
- ²¹R. Jaffiol, A. Débarre, C. Julien, D. Nutarelli, P. Tchénio, A. Taninaka, B. Cao, T. Okazaki, and H. Shinohara, *Phys. Rev. B* **68**, 014105 (2003).
- ²²M. Krause, P. Kuran, U. Kirbach, and L. Dunsch, *Carbon* **37**, 113 (1999).
- ²³R. Ahlrichs, M. Bär, M. Häser, H. Horn, and C. Kölmel, *Chem. Phys. Lett.* **162**, 165 (1989); O. Treutler and R. Ahlrichs, *J. Chem. Phys.* **102**, 346 (1995); M. V. Arnim and R. Ahlrichs, *J. Comp. Chem.* **19**, 1746 (1998); F. Weigend, *Phys. Chem. Chem. Phys.* **4**, 4285 (2002).
- ²⁴N. Lorente and M. Persson, *Phys. Rev. Lett.* **85**, 2997 (2000).
- ²⁵H. Shimotani, T. Ito, Y. Iwasa, A. Taninaka, H. Shinohara, E. Nishibori, M. Takata, and M. Sakata, *J. Am. Chem. Soc.* **126**, 364 (2004).
- ²⁶The calculated energy levels of C₈₀ do not change significantly on adsorption (cf. Ref. [10]). Particularly, the HOMO and the lowest unoccupied molecular orbital (LUMO) of the free molecule are becoming the highest occupied and the lowest unoccupied orbitals of the adsorbed Ce₂@C₈₀ (K. Muthukumar and J. A. Larsson, unpublished).
- ²⁷B. N. J. Persson, and A. Baratoff, *Phys. Rev. Lett.* **59**, 339 (1987).
- ²⁸M. Paulsson, T. Frederiksen, H. Ueba, N. Lorente, and M. Brandbyge, *Phys. Rev. Lett.* **100**, 226604 (2008).
- ²⁹N. Okabayashi, Y. Konda, and T. Komeda, *Phys. Rev. Lett.* **100**, 217801 (2008).
- ³⁰A. Gagliardi, G. C. Solomon, A. Pecchia, T. Frauenheim, A. Di Carlo, N. S. Hush, and J. R. Reimers, *Phys. Rev. B* **75**, 174306 (2007).
- ³¹E. Nishibori, M. Takata, M. Sakata, A. Taninaka, and H. Shinohara, *Angew. Chem., Int. Ed. Engl.* **40**, 2998 (2001).